Architectural Science Review

ISSN: 0003-8628 (Print) 1758-9622 (Online) Journal homepage: https://www.tandfonline.com/loi/tasr20

Improving residential building arrangement design by assessing outdoor ventilation efficiency in different regional spaces

Wei You, Jialei Shen & Wowo Ding

To cite this article: Wei You, Jialei Shen & Wowo Ding (2018) Improving residential building arrangement design by assessing outdoor ventilation efficiency in different regional spaces, Architectural Science Review, 61:4, 202-214, DOI: 10.1080/00038628.2018.1471388

To link to this article: https://doi.org/10.1080/00038628.2018.1471388

Published online: 08 May 2018.

ARCHITECTURAL SCIENCE REVIEW
2018, VOL. 61, NO. 4, 202–214
https://doi.org/10.1080/00038628.2018.1471388

Taylor & Francis
Taylor & Francis Group

Improving residential building arrangement design by assessing outdoor ventilation efficiency in different regional spaces

Wei You, Jialei Shen and Wowo Ding

School of Architecture and Urban Planning, Nanjing University, Nanjing, People's Republic of China

ABSTRACT

Using computational fluid dynamic (CFD) simulations, the correlation between residential building arrangement designs and ventilation efficiency of various outdoor spaces is explored. Three indices—purging flow rate (PFR), visitation frequency (VF) and air residence time (T_p)—are adopted to quantify the ventilation efficiency of regional outdoor spaces. Using these indices, changes in residential building lateral spacing, building length, and stagger size were investigated under the effects of different surrounding building arrays for different wind directions. The simulation results indicated that wind direction is the most important factor for improving the residential wind environment, regardless of the patterns of the surrounding building arrays. When the angle between the wind direction and the building's main façade orientation is more than 30°, the ventilation of different outdoor spaces improves. Staggered surrounding building arrays lower the spatial ventilation of the studied areas. However, this staggering does not affect the variation trend of spatial ventilation influenced by building arrangement design changes.

ARTICLE HISTORY
Received 30 September 2017
Accepted 27 April 2018

1. Introduction

Exterior space wind environments are important for urban residential areas. Weak airflow around buildings cannot efficiently dilute pollutants and remove excess heat, which influences the health and living quality of residents. One way to improve the wind environment is to use designs that are optimized for sufficient outdoor ventilation to dissipate heat and pollutants through the process of turbulent transfer. Currently, in the design process of residential building arrangements (building sizes, spacing and layout patterns), architects respond to demands regarding block shape, land use, solar access, design regulations and aesthetics (Figure 1). However, a trial-and-error method is adopted for design and optimization of outdoor wind conditions, since the correlation between practical design parameters and the wind conditions are unclear. Thus, more detailed studies are needed to explore the relationship between building arrangements and outdoor wind conditions on a micro-scale.

To explore the influence of design variations on outdoor wind conditions, it is important to select appropriate wind flow prediction methods and evaluation indices. Computational fluid dynamics (CFD) simulations and wind-tunnel tests are two of the main methods used in wind flow prediction (Blocken, Stathopoulos, and van Beeck 2016). Compared to wind-tunnel testing, the CFD method provides detailed information on the relevant flow variables in the calculation domain (i.e. 'whole-flow field data') under well-controlled conditions and without similarity constraints (Blocken et al. 2011; Blocken 2014, 2015). Therefore, the CFD method is widely used to perform urban climate studies (Toparlar et al. 2017). However, there are concerns about both the accuracy and reliability of CFD, and solution verification and validation studies are imperative. With regard to exterior space ventilation assessment, wind velocity and pollutant concentration are commonly used indices in previous studies. Ng et al. conducted a series of studies using wind velocity and pollutant concentration as indices to analyse building permeability, frontal area index and air path (Ng 2009; Ng et al. 2011; Yuan and Ng 2012; Yuan, Ng, and Norford 2014). In the last ten years, indoor ventilation indices have been developed to access ventilation efficiency in urban areas. Bady, Kato, and Huang (2008) introduced three indices from indoor performance domains into urban areas. These indices included the purging flow rate (PFR), visitation frequency (VF) and air residence time (T_p). Using these indices, the air quality of the local domains within two urban geometries (two-building urban street and building arrays) were evaluated. Kato and Huang (2009) outlined the methods for evaluating wind-induced ventilation efficiency in void spaces in built-up urban areas. They summarized six indices, which they called scales 1-6, and also summarized the local domain indices. In evaluating street ventilation in idealized city models, Hang, Sandberg, and Li (2009a, 2009b), Hang et al. (2012, 2015) and Chen et al. (2017) proposed a series of ventilation efficiency indices, including air exchange rate, mean age of air, pollutant transport rates, net escape velocity and exchange velocity.

Based on these urban ventilation performance methods, the effects of building arrangements on exterior ventilation and their related pollutant dispersion has been discussed extensively in the field of urban forms and street canyons. In these studies, ideal urban-like building groups, such as aligned and stag-

CONTACT Wowo Ding dww@nju.edu.cn

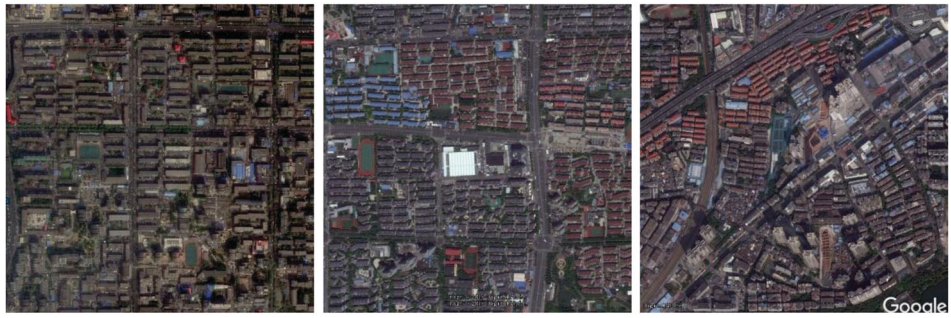

Figure 1. View of typical residential building arrangements in China: (a) Beijing, (b) Shanghai and (c) Guangzhou. (Image @ 2017 DigitalGlobe and CNES/Airbus).

gered arrays of cubes, were adopted as the geometric model. By changing the distances between building blocks and the building heights, different aspects of urban ventilation were assessed. For example, by equally varying the spacing of the buildings in the longitudinal and lateral directions, the effect of different plan area densities and frontal area densities on wind velocity (Macdonald 2000; Razak et al. 2013), pollutant dispersion (Mfula et al. 2005; Di Sabatino et al. 2007) and urban spatial ventilation efficiency (Buccolieri, Sandberg, and Di Sabatino 2010; Mei et al. 2017) were investigated. The unequal building spacing of building block arrays was also performed by Ramponi et al. (2015). It was found that widening the street improves the outdoor ventilation efficiency, whether the wind directions were oblique or perpendicular to the widened street. Hang, Li, and Sandberg (2011), Hang et al. (2012, 2015), Lin et al. (2014) and Chen et al. (2017) performed a series of studies on urban ventilation strategy within high-rise building groups. Building block arrays were also adopted to build the urban geometry model. By varying the height and numbers of building blocks in the array, different building packing densities or various urban layouts with the same building packing density were investigated. The results indicated that building arrays with height variations induce better pedestrian ventilation compared to those with a uniform height. However, these study findings focused on the characteristics of the entire city. They provide overall guidance for urban planning. More studies are needed for the following specific building arrangement designs.

At the micro-scale, street canyon ventilation is a concern for researchers, and the width/height (w/h) ratio of the street section was commonly adopted to describe the geometric characteristic of street canyons (Xie, Huang, and Wang 2006; Simoëns and Wallace 2008; Baratian-Ghorghi and Kaye 2013; Ai and Mak 2017). Based on the w/h ratio, Oke (1988) identified three types of characteristic flows. Memon, Leung, and Liu (2010) discussed the characteristic role of the w/h ratio and wind speed on air temperatures under different street canyon heating situations. They varied the w/h ratios of street sections from 0.5 to 8 and predicted the air temperatures of the street canyons with ambient wind speeds of 0.5–4 m/s. The results show that the air temperature difference between high and low w/h ratios of street canyons was the highest at night but low or negative during the day. In addition to the w/h ratio of the street section, Chan, So, and Samad (2001) and Chan, Au, and So (2003) studied the effects of different length/height (l/h) ratios of building facades on the dispersion of pollutants in different locations. The results showed that the maximum l/h ratio of building facades should be controlled within a range of 5. Yang et al. (2016) evaluated the effects of building cross-ventilation on air quality in street canyons with different building layouts (regular and staggered). Ng and Chau (2014) evaluated the influence of different configurations for two building design elements on mitigating air pollutant exposure within isolated deep canyons. Arkon and Özkol (2014) studied the effects of urban street geometries on pedestrian-level wind velocity. Additionally, several studies related to residential building arrangement designs have been conducted recently. For example, Hong and Lin (2015) simulated and compared six layout patterns of multilayer residential buildings with the same density and coverage ratio. The results showed that the building layout and orientation had a significant effect on the outdoor wind environment at the pedestrian level. Ying et al. (2013) analysed the wind environment around a building group consisting of six square high-rise buildings for six types of building layouts. Iqbal and Chan (2016) also investigated the influence of passage width on the wind flow characteristics at the re-entrant corners of cross-shaped high-rise buildings. However, most of these studies performed simulations by combining several individual buildings without considering the effects of the surrounding buildings. Additionally, for residential building arrangement design, the commonly discussed w/h ratio was restricted by sunshine conditions and land use economy. Moreover, very few systematic studies have been conducted to characterize the effects of serial practical design changes (i.e. building length, lateral spacing) on spatial wind ventilation.

This research aims to provide architects with practical knowledge for optimizing residential building arrangement in terms of the wind environment during the initial design process. Based on a previous study (You and Ding 2016), the influence of a series of design variations, including building lateral spacing, building lengths and stagger size, on ventilation efficiencies of three typical outdoor spaces are investigated under the effect of different surrounding building arrays. This study analysed the wind environment of the east China monsoon region, where the southeast monsoon wind is dominant in the summer and east and northeast winds prevail in other seasons. The wind directions adopted in this study varied from south 0° to east 90°. Slab-type and multi-storey residential buildings were selected as the study object since they account for the largest proportion of buildings in China. The CFD simulation method was adopted to

assess the influence of various designs on outdoor ventilation. The calculation tool used was ANSYS-Fluent. For the evaluation indices of ventilation efficiency, PFR, VF and T_p were employed as indicators. They reflect different aspects of pollutant dilution by wind flows in urban regional spaces.

2. Residential building configurations

2.1. Living units and combination

Configuration of residential buildings sizes (width W, depth D and Height H) involves the selection of a living unit and their combination. Liu and Ding (2012) summarized different types of living units in newly built residential districts in China. Three types of living units (U1, U2, U3) were selected to perform the unit combinations, as shown in Figure 2(a). They are commonly used in residential building design and meet the living demands of different families. Building length W was determined by the combination of the living units, which were divided into two and multi-unit combinations (Figure 2(b)). Considering the economy, living units with larger areas (i.e. U3) were selected as side units in two-unit and multi-unit groups. Therefore, the minimum W was set as 28.8 m. The depth D of the building equals the living unit (D = 12 m). The building height H was set as 18 m with six stories. The undulation of balconies on the southward façade was considered as a uniform single plane to simplify the computation.

2.2. Calculated residential buildings group setup

Due to the design considerations of function, sunshine, fire protection and economical use of land resources, residential areas in China share a noticeable fabric characteristic, as shown in Figure 1. Based on the patterns of existing residential areas, two types of 3 × 3 striped building groups were established as the CFD simulation geometric model, considering the effect

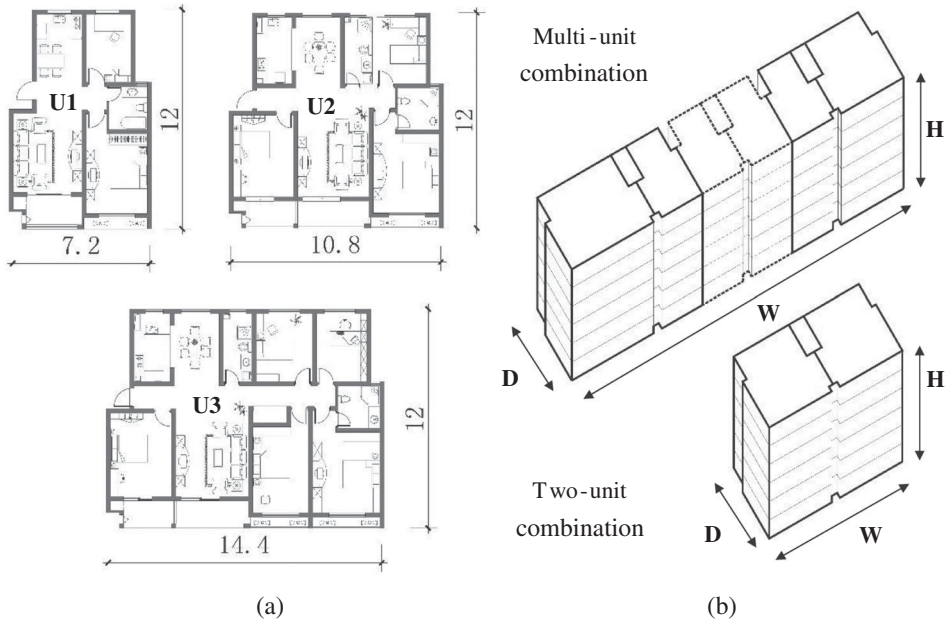

Figure 2. Living units and unit combinations in a residential building, (a) Living units (Unit: m); (b) Unit combinations.

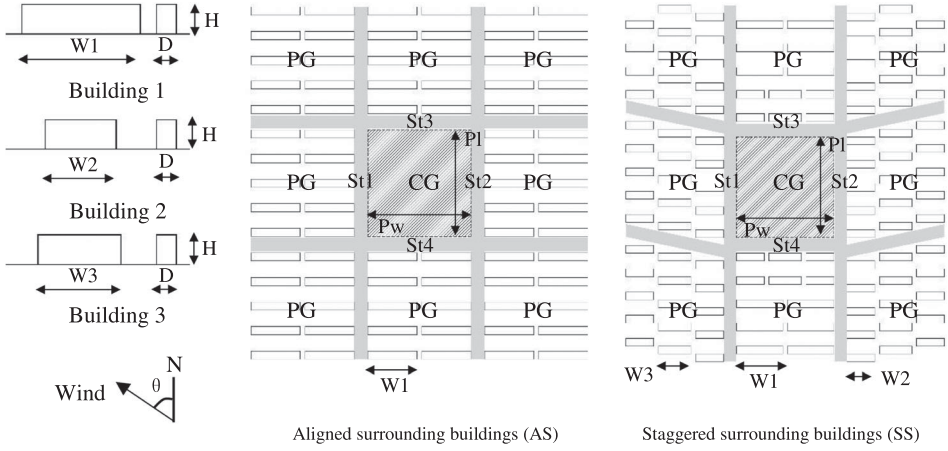

Figure 3. Building configurations and surrounding building layouts (W1 = 72 m, W2 = 43.2 m, W3 = 50.4 m, D = 12 m, H = 18 m).

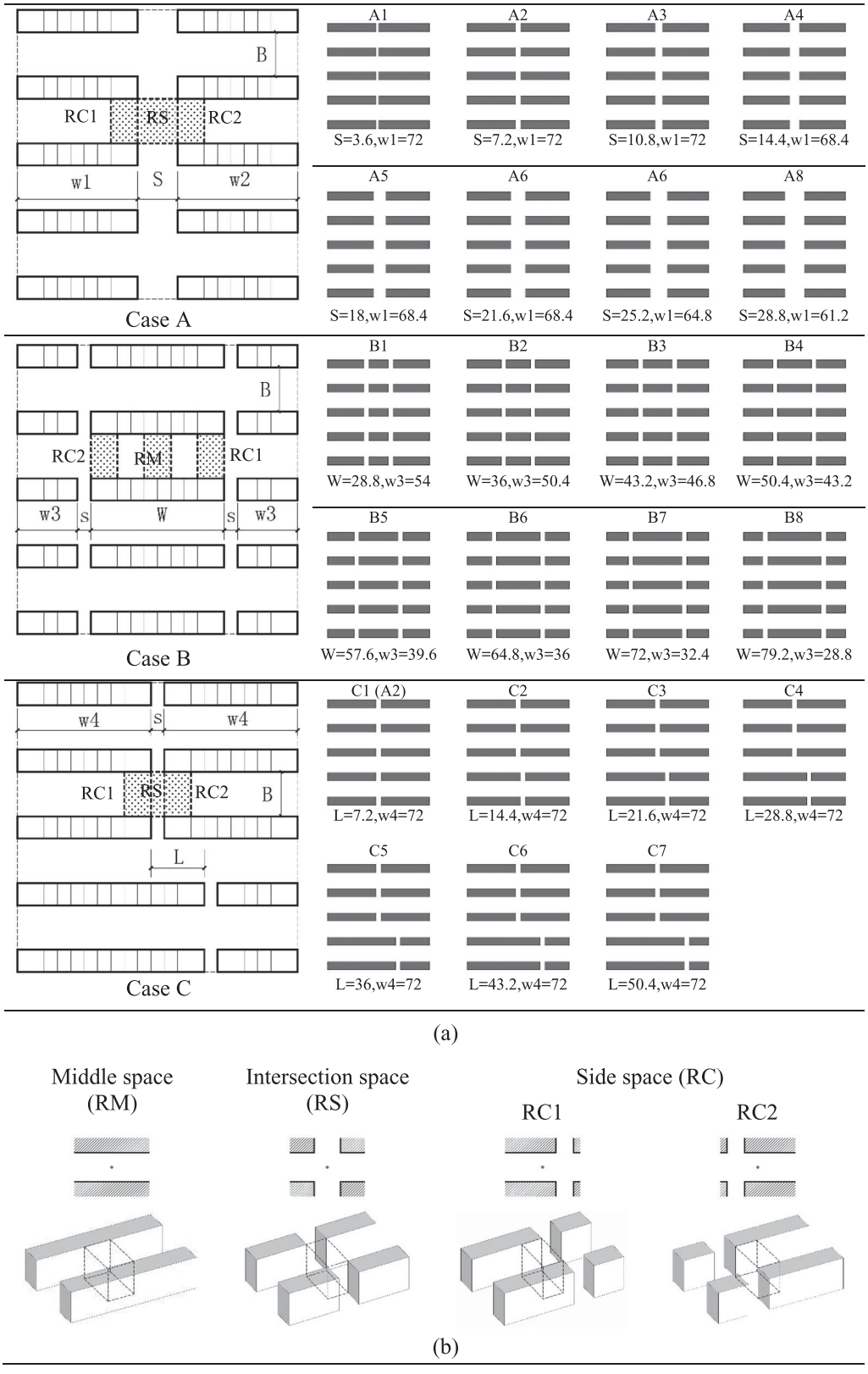

Figure 4. (a) Design changes and studied domains (Unit: m); (b) Space classification of the studied domains.

of surrounding buildings with aligned (AS) and staggered (SS) arrays (Figure 3). The central group (CG) provided variation in the configuration analysis, and the peripheral groups (PG) set the environmental conditions. Design variations of the central groups will be introduced in section 2.3. The sizes (Pw, Pl) of the CG were 156 m. The widths of the four streets (St1-St4) were determined to be 20 m, which conforms to the current design code (GB50180-93 2002).

2.3. Building arrangement design variation

Three design variations were investigated in this study, as shown in Figure 4(a). Case A denotes the varying lateral spacing of buildings, Case B represents the varying building lengths, and Case C represents varying the staggering of the building layout. The longitudinal spacing B was fixed at 24 m. Ventilation efficiency of three typical spaces were evaluated (Figure 4(b)), naming them RM space, RS space and RC space. The RM space was the outdoor middle space of the investigated building. The RS space represents the outdoor intersection space. The RC (RC1 and RC2) space refers to the outdoor side space that adjoins the RS space. The domain volumes of RM and RC were invariant, with a uniform size of 14.4 m wide and 24 m long. The volume of the RS space varied as the building spacing changed. The domain height was from the ground to building height H. The spatial ventilation of these three spaces within different cases were investigated under south (θ = S 0°), southeast (θ = SE 45°) and east (θ = E 90°) wind directions.

3. Ventilation efficiency performance

Three ventilation efficiency indices were adopted in this study: the purging flow rate (PFR), visitation frequency (VF) and air residence time (T_p), reflecting the capacity to remove pollutants by airflow, wind recirculation, and air freshness, respectively. These indices are new outdoor ventilation evaluation criteria, which were recently developed for the indoor performance area. It is difficult to determine the specific values of the optimal wind environment for these indices. However, using a series of design variation case simulations, the influence trend and inflexion point of the design sizes on these evaluation indices could be obtained. Within the threshold determined by the inflexion point, the optimal residential wind environment was identified, as more wind reaching the regional spaces dissipates heat and pollutants, and less wind recirculates in these regions.

Currently, PFR is a commonly used index in urban street ventilation studies (Lin et al. 2014; Hang et al. 2013; 2015; Shen et al. 2017; Mei et al. 2017), though the concept was originally introduced to assess the effective airflow rate of flushing a room. PFR is defined as the effective airflow rate required to purge the air pollutants from the domain, and it reflects the capacity at which the wind removes the pollutants from the domain. If a uniform contaminant source is fixed in the studied local domain, the PFR (m^3/s) of that domain is calculated as:

$$PFR = \frac{S_c \times Vol}{\langle C \rangle} = \frac{S_c \times Vol}{\int_{Vol} Cdxdydz/Vol} \quad (1)$$

where S_c denotes the pollutant generation rate (kg/ m^3·s), $< C >$ is the spatially averaged concentration in the entire studied domain (kg/m^3), and *Vol* is the domain volume (m^3).

In addition to the level of the pollutant concentration, the pollutant behaviour within the domains was investigated. VF is an index to measure the pollutant behaviour. It describes the number of times a particle returns, circulates and remains inside the domain. VF = 1 indicates a particle remains only once within the domain. VF = 2 means that a particle, which is transported outside, returns once to the domain due to the recirculation flow. The VF (time) can be calculated as:

$$VF = 1 + \frac{\Delta q_p}{S_c \times Vol} \quad (2)$$

where Δq_p is the inflow flux of pollutants into the domain (kg/s). It consists of the convection and turbulent diffusion portions of the inflow flux. Bady, Kato, and Huang (2008) indicated that the inflow flux in the street canyon was almost exclusively affected by the value of the mean part of the flux, while the turbulent part of the flux had no considerable influence.

T_p represents the air age concept of the local domain. It is a measure of the air freshness and thus the dilution capability of wind within the domain. T_p is defined as the time it takes once a particle enters or is generated in the domain until it leaves the domain. The T_p is the average time a pollutant stays in the local domain for one visitation. Multiplying T_p by VF gives the total average staying time (lifespan of a contaminant particle) in the local domain. Therefore, the equation for T_p is:

$$T_p = \frac{Vol}{PFR \times VF} \quad (3)$$

These indices can be calculated using the CFD approaches. The calculation process consists of three steps as follows. First, calculate and obtain the flow field within the distribution area. Second, determine the pollution source of the local domain according to the study demands and calculate the concentration distribution of pollutants with the mass transfer equation. Third, calculate the ventilation efficiency indices via various calculation formulas.

4. CFD modelling set-up

4.1. Turbulence models for urban airflow modelling

For CFD modelling approaches, steady Reynolds-averaged Navier Stokes (RANS) and large eddy simulation (LES) approaches are commonly compared and discussed by researchers. LES performs better than RANS at predicting turbulent flows. However, LES consumes more computational time than does the RANS approach, and the turbulent model setup is also more complex (Tominag and Stathopoulos 2010; Moonen, Dorer, and Carmeliet 2011; Salim et al. 2011; Liu and Niu 2016). Regarding accuracy, the simulation results of the RANS approach are sufficient if urban wind prediction focuses on mean wind speed rather than on effective wind speed. Lin et al. (2014) performed a sensitivity study of various RANS approaches by comparing them with experimental data. Simulation results showed that RANS approaches provide data that agree with the experiments and further indicated that the standard k-ϵ model was better in simulating stream-wise velocity profiles, turbulent kinetic energy profiles and vertical velocity below street roofs than the other three models. Many previous studies also utilized the standard k-ϵ model to predict the urban wind flows (Bady, Kato, and Huang 2008; Hang, Sandberg, and Li 2009a, 2009b, 2015; Buccolieri, Sandberg, and Di Sabatino 2010, 2015). Considering that RANS turbulence models are less time-consuming and this study focused on mean wind velocity, the steady RANS approach with standard k-ϵ turbulence model was adopted in this study.

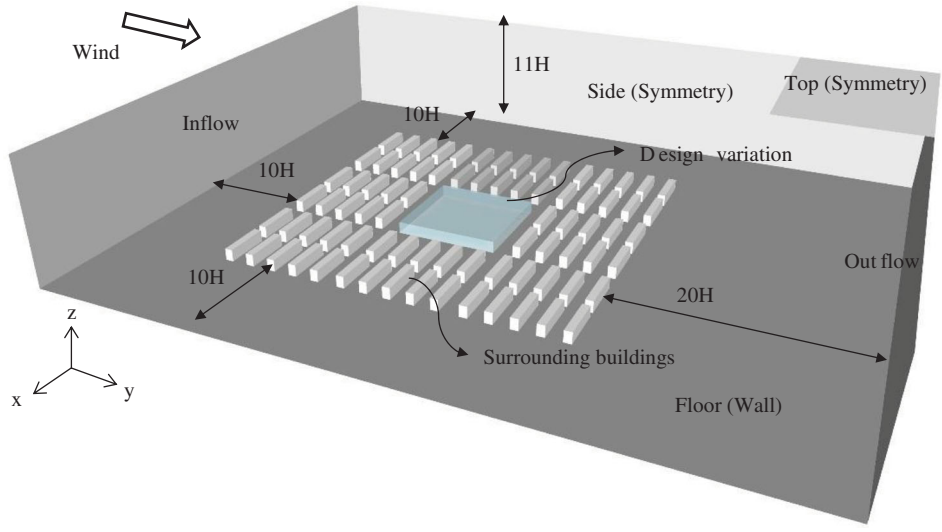

Figure 5. Computational domain and boundary conditions in CFD simulations (H: building height).

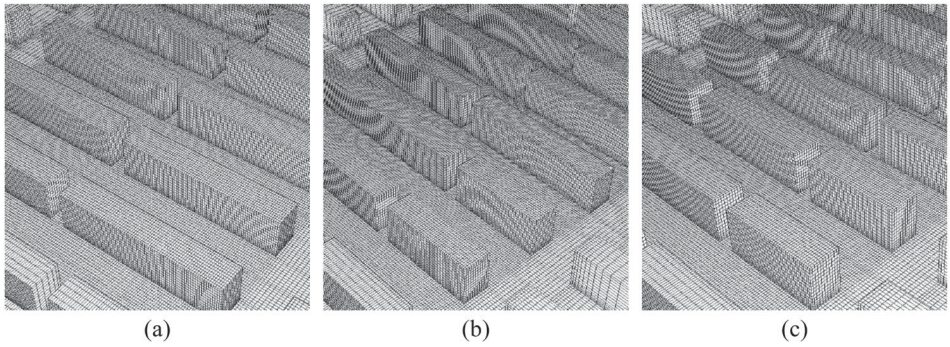

Figure 6. Gird resolution in the computational domain for (a) Case A2; (b) Case B5; (c) Case C5.

4.2. Computational domain and grid

The computational domain and mesh resolution fulfil the major simulation requirements, as recommended by the AIJ (Architectural Institute of Japan) guideline (Tominaga et al. 2008) and the COSTA (European Cooperation in Science and Technology) action (Franke et al. 2011). The computational domain sizes are shown in Figure 5. The lateral and inflow boundaries were set to 10 H away from the building groups, where H was the uniform building height. The outflow boundary was 20 H away from the building groups, and the height of the computational domain was 11 H. Hexahedral elements were built in the computational domain, as shown in Figure 6. The minimum grid control in direction z was 0.028 H, the minimum grid control in the x-y direction was 0.056 H, and the maximum expansion factor between grids was below 1.25.

4.3. Boundary conditions and solver settings

The inlet profiles presented by Richards and Hoxey (1993) were set as the inflow boundary conditions. The vertical wind velocity profile (U) was calculated as:

$$U(z) = \frac{u^*_{ABL}}{\kappa} \ln\left(\frac{z + z_0}{z_0}\right) \tag{4}$$

where U_{ABL}* is the atmospheric boundary layer friction velocity (m/s). z_0 is the aerodynamic roughness length (m), z is the height coordinate (m), and κ is the von Karman constant, which was determined to be 0.4. The turbulent kinetic energy profile (k) and turbulent dissipation rate profile (ϵ) were calculated as:

$$k(z) = \frac{{u^*_{ABL}}^2}{\sqrt{C_\mu}} \tag{5}$$

$$\varepsilon(z) = \frac{{u^*_{ABL}}^3}{\kappa(z + z_0)} \tag{6}$$

where C_μ is a constant (0.09). Symmetry boundary conditions, required to enforce a parallel flow, were imposed on the top and lateral sides of the domain. At the outlet boundary of the domain, a pressure-outlet condition was used. No-slip wall boundary conditions were used for all solid surfaces.

The SIMPLE algorithm was utilized for pressure-velocity coupling. Pressure interpolation was in second-order accuracy. For both the convection terms and the viscous terms of the governing equations, second-order discretisation schemes were used.

4.4. Validation of the CFD simulation

The implemented CFD simulation method was validated by the author in a previous study (You et al. 2017). This paper is a further study based on that preliminary investigation of the effects

of residential design on regional spatial ventilation. The validation study included grid sensitivity analysis and experimental verification. The grid sensitivity analysis was performed by comparing the distributions of wind velocity with the three grids (coarse, basic and fine grid). The principle of basic gird meshing was in accordance with this study. The results showed that the profiles of wind velocity calculated with the basic grid generally agreed with those calculated using the fine grid, and errors caused by the grid resolutions did not have a noticeable effect on the numerical results. Experimental verification was performed by comparing the CFD simulation results with a wind-tunnel experiment of similar strip-type building groups. Since the experimental building group was different from that used in this study, we built an extra building model with inlet boundary and geometry conditions identical to the wind-tunnel tests. The numerical predictions were consistent with the experimental results, especially for the wind profile at upwind regions. The wind profile at a location with a recirculating flow region was slightly lower than the experimental results. It was similar to previous studies (Tominaga et al. 2004; Tominag and Stathopoulos 2010), which indicated that in the wake region behind the building, the predicted wind speed is underestimated.

5. Simulation results and analysis

5.1. Influence of wind direction changes

Two typical cases (Case A2 and Case B4) with two types of surrounding buildings were selected as the objects for assessing exterior spatial ventilation under different wind directions (from a south direction (θ = S 0°) to east (θ = E 90°), with an interval of 22.5°).

Figure 7 shows the influence of wind direction on spatial ventilation under the effect of the surrounding buildings. From the figures, it can be seen that ventilation efficiencies of different spaces improved as the wind direction changed from the south (θ = S 0°), which was perpendicular to the main (long) building façade, to the east (θ = E 90°), which was parallel to the main building façade. This was due to the strip-shaped spatial structure, which had a duly north–south façade directed ventilation corridor due to the sunlight requirement. As the wind direction changed from perpendicular to parallel to the ventilation corridor, the wind flow entering the space between the residential buildings increased significantly. However, the variation trends differed slightly for different ventilation indices. In subplot (a) and (b), the PFRs initially increased rapidly, then slowed when the wind direction θ was over 45°. However, when the wind direction θ changed to 22.5°, the VFs and T_ps decreased. Then, the descend range dropped. This was due to the meanings of these indices. PFR refers to the fresh airflow quantity entering the domain, while VF represents the reversal flow phenomena. When the direction changed from 0° to 22.5°, the VFs decreased from above 1.3 to below 1.1, which reflected that the recirculation of wind flows weakening. Affected by the VFs, the varying point of T_ps also appeared at wind direction 22.5°.

As the wind direction changed, the variation trend of VFs within the intersection space (RS) differed from that within the other spaces. In subplot (a), although the VFs of the RS spaces decreased as the wind direction changed from θ to 22.5°, the decrease was slow, with a variation range below 6%. This was

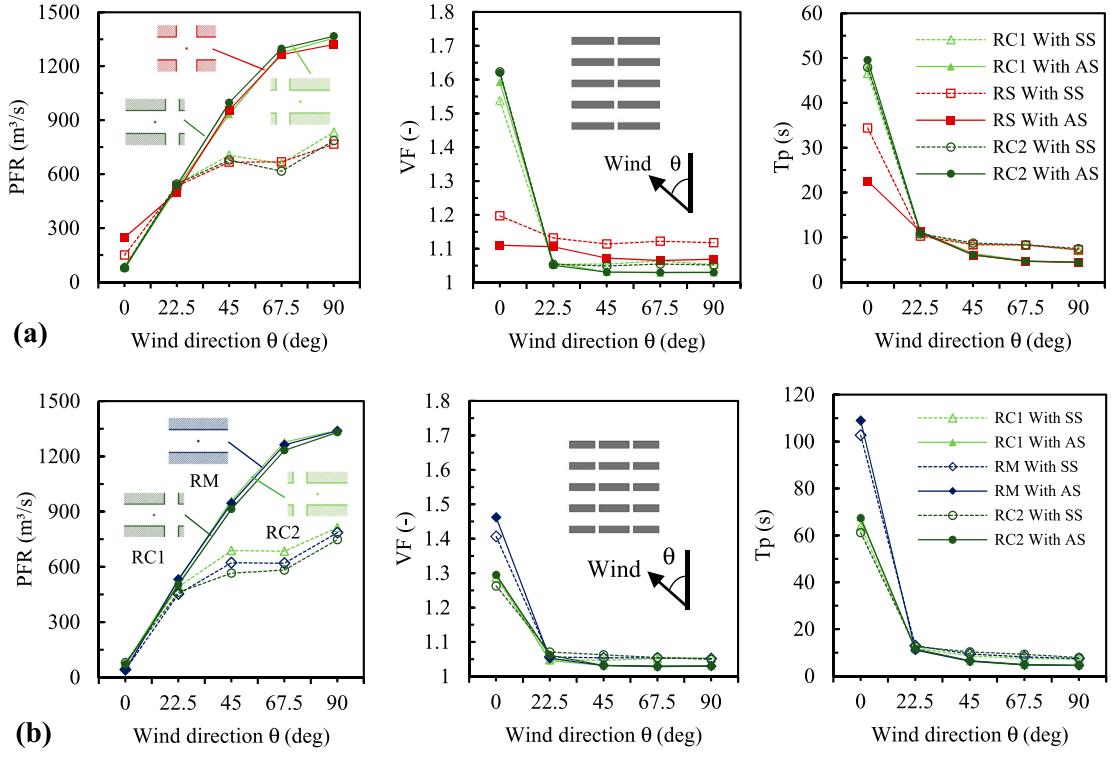

Figure 7. Influence of wind direction changes on spatial ventilation efficiency of (a) Case A2, (b) Case B4, with the effect of aligned (AS) and staggered (SS) surrounding building arrays.

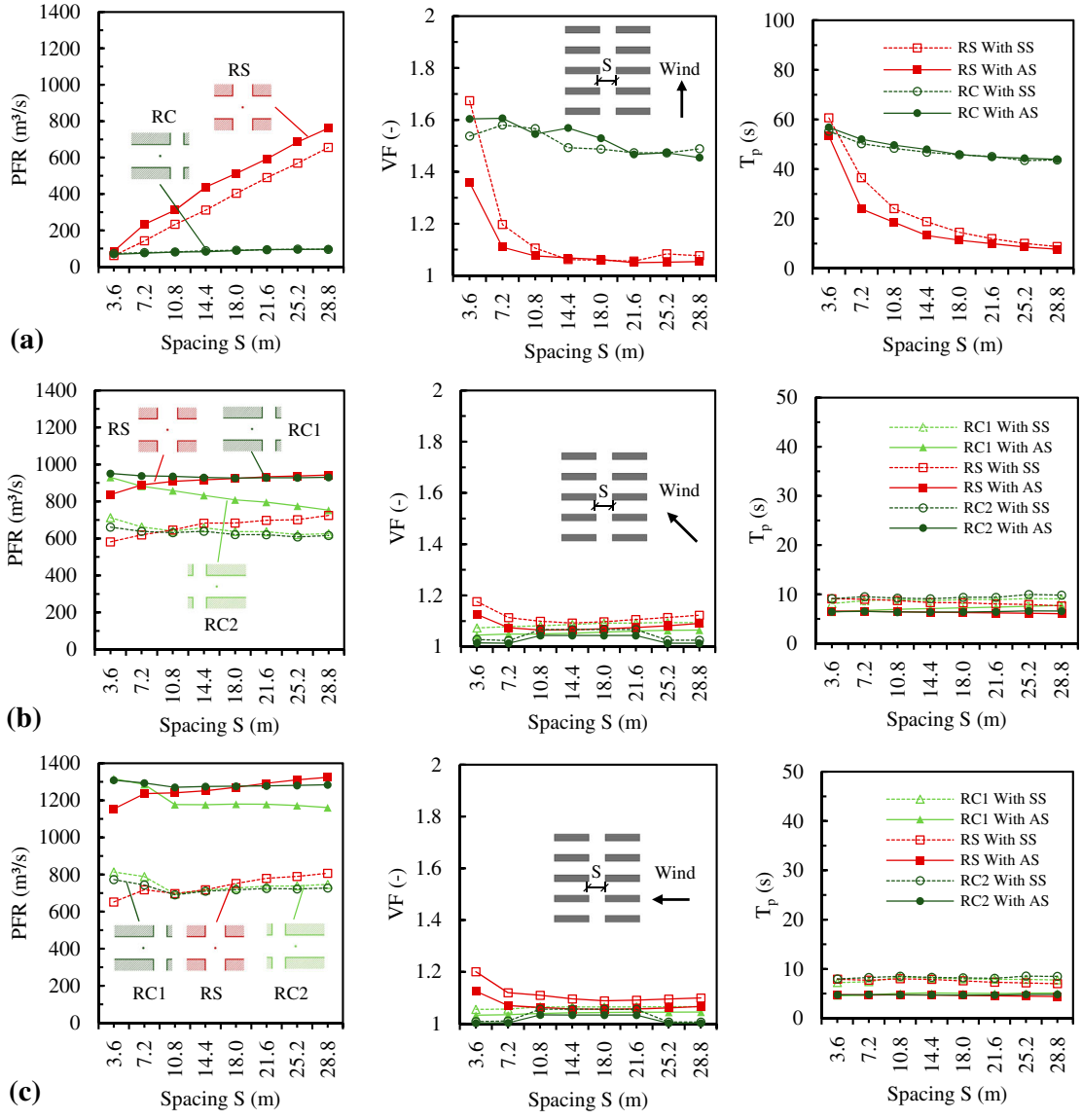

Figure 8. Influence of lateral spacing changes on spatial ventilation efficiency under (a) south 0°, (b) southeast 45° and (c) east 90° wind directions, with the effect of aligned (AS) and staggered (SS) surrounding building arrays.

due to the characteristics of the spatial geometry. In side spaces (RC1 and RC2) and the middle space (RM), the north and south façade walls directed the wind flow, which decreased the VFs when the wind direction was oblique to the north/ south façade wall. However, in the RS space, the wind flowed from the southeast or east direction striking the corners of the surrounding buildings. This caused the reversal of flow in the RS space.

The arrangement pattern of the surrounding buildings also had an effect on the spatial ventilation. Compared to the surrounding buildings with aligned arrays, staggered surrounding building arrangements lowered the spatial ventilation efficiency in the studied areas. The PFRs of different spaces were higher within the aligned surrounding building arrays than the PFRs within staggered surrounding building arrays. However, the VFs of different spaces were slightly lower within the aligned surrounding buildings than within the staggered surrounding buildings. This was because the staggered building arrays blocked the wind flow path and the air was exchanged by turbulent flows.

5.2. Lateral spacing change

The effects of building lateral spacing changes on ventilation efficiency indices are displayed in Figure 8. From the simulation results, it was found that widening lateral spacing improved the ventilation performance of the varying intersection space (RS) and its adjacent side spaces (RC1 and RC2). In subplot (a), (b) and (c), as the lateral spacing increased, the variations of PFRs in the RS spaces differed greatly under different wind directions. This was due to the definition of PFR. The PFR represents the supplied 'fresh' airflow volume that is adopted to purge air pollutants from the domain. Many studies (Peng and Davidson 1997; Bady, Kato, and Huang 2008; Lim, Ito, and Sandberg 2013; Hang et al. 2015) have indicated that PFR is dependent on the volume of the target domain. However, it may have more dependence on the inlet airflow opening size. Therefore, it was expected that under the south wind direction, the PFRs would increase with an almost linear relationship to the lateral spacing (Figure 8(a)), while the increases were limited under the southeast and east

wind directions (Figure 8(b,c)). The improvement of the ventilation performance of the RS spaces was reflected by combining VF and T_p. In subplots (a), it was found that VFs and T_ps decreased as the building spacing increased, especially when the building spacing changed from 3.6 m (A1) to 7.2 m (A2). The variation ranges of VF and T_p reached 18.3% and 65.2%, under the aligned surrounding buildings conditions. This finding was due to the improvement of airflow recirculation, which was reflected by index VF.

In evaluating the RC spaces, in which the space volume was constant, PFR was an efficient index. Under a southern wind direction (Figure 8(a)), the PFR increased by 42% and 33% for staggered and aligned surrounding building conditions, respectively, as the lateral spacing changed from 3.6 m (A1) to 28.8 m (A8). This improvement was also found by calculating VF and T_p, both of which decreased. Under the southeast and east wind directions (Figure 8(b,c)), ventilation of spaces RS and RC1 were also improved by broadening the lateral spacing of the buildings, but the ventilation efficiency of the RC2 space decreased. In Figure 8(b), the PFR of the RC2 space decreased by 20% under the aligned surrounding building condition. This may be because the wind flow entered from the east side into the RC2 space, and as the lateral spacing increased, the RC2 space gradually moved away from the upstream flow, which caused the decrease in the wind velocity in the domain.

Different surrounding building arrays also affected spatial ventilation. However, the different arrays of surrounding buildings had only a quantitative influence on ventilation efficiency (i.e. lower spatial ventilation efficiency was found with staggered surrounding buildings) and did not influence the variation trend.

5.3. Building length change

The ventilation efficiency of the outdoor middle space (RM) and side spaces (RC1 and RC2), were investigated under the effect of residential building length change for different wind directions. The PFR, VF and T_p of these spaces under the southern wind

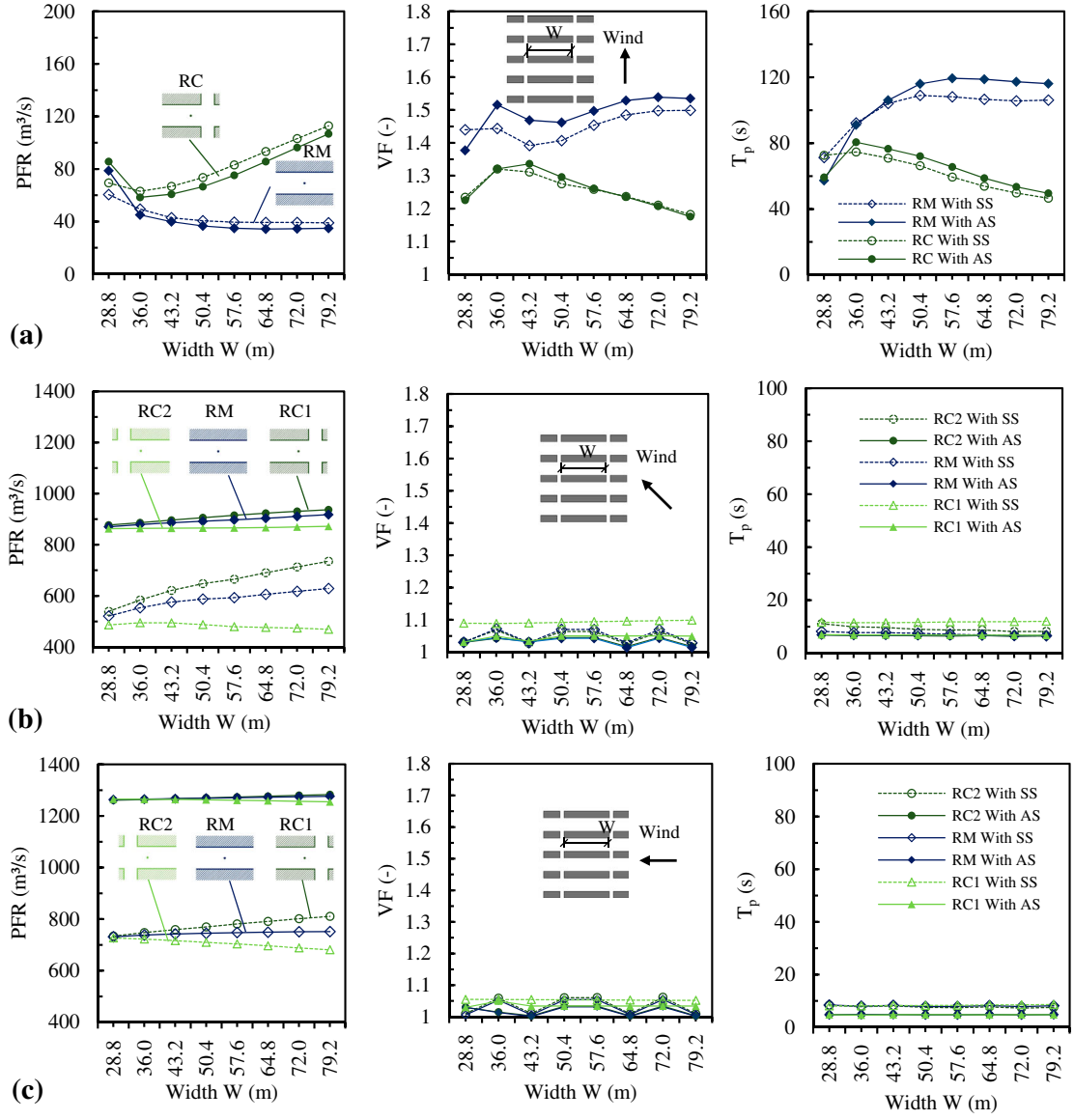

Figure 9. Influence of building length changes on spatial ventilation efficiency under (a) south 0°, (b) southeast 45° and (c) east 90° wind directions, with the effect of aligned (AS) and staggered (SS) surrounding building arrays.

direction (θ = S 0°), southeast wind direction (θ = SE 45°) and eastern wind direction (θ = E 90°) are shown in Figures 9(a–c). From the simulation results, it was found that building length change influenced the outdoor spatial ventilation of the residential area, especially when the wind direction was approximately perpendicular to the main (long) building façade. In subplot (a), when the wind direction was θ = S 0°, as the building length W increased, the PFR of the RM space decreased. Considering Case B1 (W = 28.8 m) and Case B8 (W = 79.2 m) as examples, the PFRs of the RM spaces decreased by 55% and 35%, respectively, under the surrounding buildings with aligned and staggered arrays. This indicates a decrease in the spatial purging capacity for air pollutants. The VF of the RM space increased slightly, which reflects the strengthening of the wind flow recirculation in these domains. Under these combined effects, the varying inflexion point of the average staying time (T_p) appeared at building length W = 50.4 m (B4). When building length W increased from 28.8 m to 50.4 m, the T_p of the RM space increased by 102% and 53% under aligned and staggered surrounding buildings, respectively. The T_p remained approximately constant as the building length W increased. This was due to the decrease of wind flow entering the RM space as the building length increased. This result verified our previous study, which indicated that increasing building length might not be beneficial for the ventilation of the middle living units of residential buildings (You et al. 2017). Conversely, the PFRs of the RC spaces (mean value of RC1 space and RC2 space) decreased slightly, then increased. In addition, the VF and T_p of the RC space increased, then decreased. However, the reason for this may not be completely due to the influence of building length increases. Part of the reason may be that the RC spaces gradually approached the east and west streets (St1 and St2) of the study area, which led to the acceleration of the wind speed in the RC spaces. Meanwhile, less recirculation flow occurred in these domains.

When the wind direction turned gradually, becoming parallel to the building's main façade, spatial ventilation was less influenced by the changes in building length. Figure 9(b,c) shows

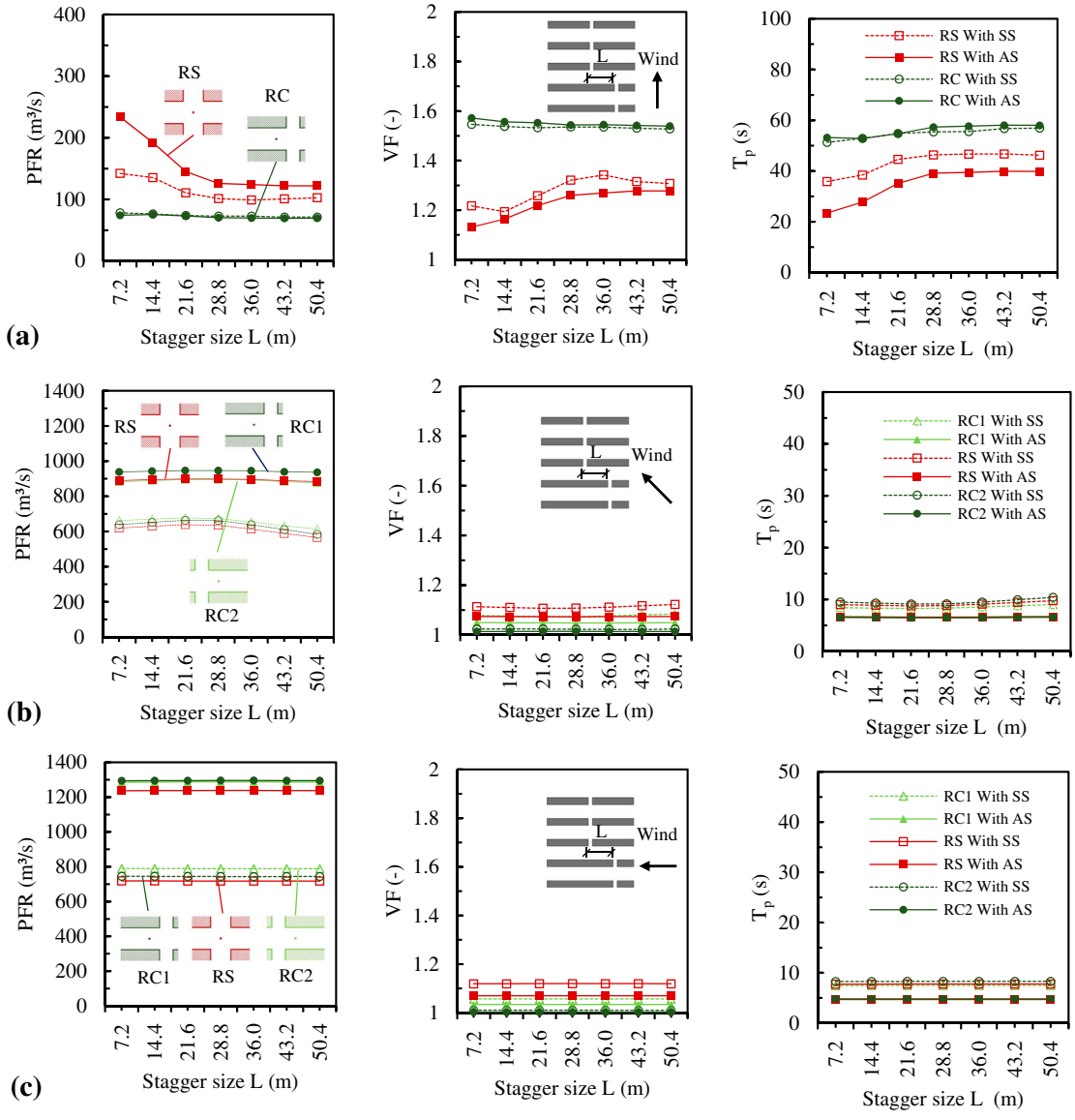

Figure 10. Influence of building stagger changes on spatial ventilation efficiency under (a) south 0°, (b) southeast 45° and (c) east 90° wind directions, with the effect of aligned (AS) and staggered (SS) surrounding building arrays.

the effects of building length variations on ventilation efficiency of RM and RC spaces, under the southeast and eastern wind directions. From the figures, it can be seen that, when the surrounding buildings had staggered arrays, the variation of PRF and T_p within these spaces reached 35% and 26% for the southeast (θ = SE 45°) wind direction, while the variation of those within these spaces only reached 10% and 9% for the east θ = E 90° wind direction. This might be due to the characteristic change in airflow turbulence. When the surrounding buildings had aligned arrays, the effects of building length variation on different spatial ventilation could be neglected, with the variations of PFR and T_p all below 6% when the wind direction was greater than 45°.

Similarly, as building spacing changed, surround buildings also did not influence the variation trend as the building length changed. However, the variation was more obvious when the surrounding buildings were staggered compared to arrays of aligned surrounding buildings.

5.4. Changes in location staggering

Figure 10 shows the influence of changes in the building staggering on the ventilation efficiency of the intersection space (RS) and side spaces (RC1 and RC2). Similar to the building length change, the ventilation efficiencies of these spaces were affected more by changes in the building staggering under the south wind directions. In Figure 10(a), when the staggering distance increased from 0 m (C1) to 28.8 m (C4), PFRs of the RS spaces decreased by 46% and 29%, respectively, for the aligned and staggered surrounding building conditions. This decrease was due to the staggered building arrangement, which blocked the airflow path in the RS space. When the staggering distance increased from 28.8 m (C4) to 50.4 m (C7), the decrease of PFRs remained approximately constant with variation below 3%. The similar inflexion points were also obtained using the VF and T_p analysis. Ventilation efficiency of the RC spaces was also affected by changes in the building staggering, but the effects were limited compared to the RS space. Additionally, considering C1 and C4, for example, regarding the aligned and staggered surrounding building conditions, PFRs of the RC spaces decreased by 5% and 7%, VFs of the RC spaces decreased by 2% and 1%, and T_ps of the RC spaces increased by 8% and 9%, respectively.

Under southeast (θ = SE 45°) and east (θ = E 90°) wind conditions (Figure 10(b,c)), the effects of changes in building staggering on spatial ventilation were limited. As the building staggering distance increased, the PFRs of the different domains decreased slightly under wind direction θ = SE 45° for the staggered surrounding building condition (Figure 10(b)). With other conditions, the ventilation efficiency indices remained approximately constant, with a variation range below 8%.

6. Conclusion

This paper assessed the effects of serial residential building arrangement designs on the ventilation efficiencies of typical outdoor spaces under different wind directions. Design variations, such as lateral spacing, building length and the stagger of the building layout, were investigated under the effects of two different surrounding building arrays using CFD simulation techniques. PFR, VF and T_p were adopted to perform the analysis and obtain the inflexion points of the influence curve, which were used to control the design size for better wind conditions. The conclusions are as follows:

(1) Wind direction and residential building orientation is an important factor for improving the residential wind environment, regardless of the patterns of the surrounding building arrays. The main orientation and local prevailing wind direction should be seriously considered in the design process. For the east China monsoon region, where south, southeast and east wind is predominant in most seasons, the optimal orientation of building groups for wind environment optimization are formed southwest 30° to south, as the wind goes through the north–south façade directed ventilation corridor and improves the ventilation efficiency of different spaces.
(2) Lateral spacing variation has an influence on the ventilation efficiency of the varying intersection space (RS) and its adjacent side spaces (RC1 and RC2), especially when the wind direction is perpendicular to the main building façade. For the slab-type and multi-storey residential buildings, when the lateral building spacing increased to more than 7 m, the ventilation efficiency of these spaces improved noticeably.
(3) Increasing building length will not benefit the ventilation performance of the outdoor middle space (RM). From simulation results, residential building length could be restricted to 60 m (about three residential-unit combinations of dwellings). This might lead to an increase in wind flow into the middle spaces, which is beneficial for the middle living units.
(4) Changes to building staggering influences the ventilation efficiency of the outdoor intersection space (RS). Increasing the building staggering blocks the airflow path in the RS space, which decreases the spatial ventilation. The variation inflexion point of the staggering length is approximately 25 m.
(5) Surrounding building arrangement patterns also have an effect on spatial ventilation. Compared to the surrounding buildings with aligned arrays, staggered surrounding building arrangements lowered the spatial ventilation efficiency in the studied areas. However, this staggering did not affect ventilation variation trend of spaces, which is influenced by building arrangement design changes.

This research analysed the influence of several design changes on the ventilation of outside spaces. Due to urban form complexity, the conclusions are constrained to the studied patterns. In future research, additional numerical simulations should be performed to discuss additional building arrangement designs. For example, variations in building heights and leisure square designs will also be discussed in subsequent studies.

Acknowledgements

The authors would like to acknowledge the valuable comments and discussions provided by Dr. Zhi Gao, Dr. Jian Hang and Dr. Zhi Chen on the simulation technique and ventilation efficiency performance. The authors also

would like to acknowledge DigitalGlobe and Centre National d'Etudes Spatiales (CNES) for providing the images of view picture of typical residential building arrangements in China.

Disclosure statement

No potential conflict of interest was reported by the author(s).

Funding

The National Key Research and Development Programme of China supported this work under [grant number: 2017YFC0702502]; and the National Natural Science Foundation of China under [grant numbers: 51508262 and 51538005].

References

Ai, Z. T., and C. M. Mak. 2017. "CFD Simulation of Flow in a Long Street Canyon Under a Perpendicular Wind Direction: Evaluation of Three Computational Settings." *Building and Environment* 114: 293–306.

Arkon, C. A., and Ü Özkol. 2014. "Effect of Urban Geometry on Pedestrian-Level Wind Velocity." *Architectural Science Review* 57 (1): 4–19.

Bady, M., S. Kato, and H. Huang. 2008. "Towards the Application of Indoor Ventilation Efficiency Indices to Evaluate the Air Quality of Urban Areas." *Building and Environment* 43: 1991–2004.

Baratian-Ghorghi, Z., and N. B. Kaye. 2013. "The Effect of Canyon Aspect Ratio on Flushing of Dense Pollutants From an Isolated Street Canyon." *Science of the Total Environment* 443: 112–122.

Blocken, B. 2014. "50 Years of Computational Wind Engineering: Past, Present and Future." *Journal of Wind Engineering and Industrial Aerodynamics* 129: 69–102.

Blocken, B. 2015. "Computational Fluid Dynamics for Urban Physics: Importance, Scales, Possibilities, Limitations and ten Tips and Tricks Towards Accurate and Reliable Simulations." *Building and Environment* 91: 219–245.

Blocken, B., T. Stathopoulos, J. Carmeliet, and J. L. M. Hensen. 2011. "Application of Computational Fluid Dynamics in Building Performance Simulation for the Outdoor Environment: An Overview." *Journal of Building Performance Simulation* 4 (2): 157–184.

Blocken, B., T. Stathopoulos, and J. P. A. J. van Beeck. 2016. "Pedestrian-level Wind Conditions Around Buildings: Review of Wind-Tunnel and CFD Techniques and Their Accuracy for Wind Comfort Assessment." *Building and Environment* 100: 50–81.

Buccolieri, R., P. Salizzoni, L. Soulhac, V. Garbero, and D. Di Sabatino. 2015. "The Breathability of Compact Cities." *Urban Climate* 13: 73–93.

Buccolieri, R., M. Sandberg, and D. Di Sabatino. 2010. "City Breathability and Its Link to Pollutant Concentration Distribution Within Urban-Like Geometries." *Atmospheric Environment* 44: 1894–1903.

Chan, A. T., W. T. W. Au, and E. P. S. So. 2003. "Strategic Guidelines for Street Canyon Geometry to Achieve Sustainable Street air Quality—Part II: Multiple Canopies and Canyons." *Atmospheric Environment* 37: 2761–2772.

Chan, A. T., E. P. S. So, and S. C. Samad. 2001. "Strategic Guidelines for Street Canyon Geometry to Achieve Sustainable Street air Quality." *Atmospheric Environment* 35: 4089–4098.

Chen, L., J. Hang, M. Sandberg, L. Claesson, S. Di Sabatino, and H. Wigo. 2017. "The Impacts of Building Height Variations and Building Packing Densities on Flow Adjustment and City Breathability in Idealized Urban Models." *Building and Environment* 118: 344–361.

Di Sabatino, D., R. Buccolieri, B. Pulvirenti, and R. Britter. 2007. "Simulations of Pollutant Dispersion Within Idealized Urban-Type Geometries with CFD and Integral Models." *Atmospheric Environment* 41: 8316–8329.

Franke, J., A. Hellsten, H. Schlünzen, and B. Carissimo. 2011. "The COST732 Best Practice Guideline for CFD Simulation of Flows in the Urban Environment – A Summary." *International Journal of Environment and Pollution* 44 (1–4): 419–427.

GB50180-93. 2002. *Code of Urban Residential Areas Planning & Design*. Beijing: China Architecture and Building Press. (in Chinese).

Hang, J., Y. G. Li, and M. Sandberg. 2011. "Experimental and Numerical Studies of Flows Through and Within High-Rise Building Arrays and Their Link to Ventilation Strategy." *Journal of Wind Engineering and Industrial Aerodynamics* 99: 1036–1055.

Hang, J., Y. G. Li, M. Sandberg, R. Buccolieri, and S. Di Sabatino. 2012. "The Influence of Building Height Variability on Pollutant Dispersion and Pedestrian Ventilation in Idealized High-Rise Urban Areas." *Building and Environment* 56: 346–360.

Hang, J., Z. W. Luo, M. Sandberg, and J. Gong. 2013. "Natural Ventilation Assessment in Typical Open and Semi-Open Urban Environments Under Various Wind Directions." *Building and Environment* 70: 318–333.

Hang, J., M. Sandberg, and Y. G. Li. 2009a. "Age of air and air Exchange Efficiency in Idealized City Models." *Building and Environment* 44: 1714–1723.

Hang, J., M. Sandberg, and Y. G. Li. 2009b. "Effect of Urban Morphology on Wind Condition in Idealized City Models." *Atmospheric Environment* 43: 869–878.

Hang, J., Q. Wang, X. Y. Chen, M. Sandberg, W. Zhu, R. Buccolieri, and D. Di Sabatino. 2015. "City Breathability in Medium Density Urban-Like Geometries Evaluated Through the Pollutant Transport Rate and the Net Escape Velocity." *Building and Environment* 94: 166–182.

Hong, B., and B. Lin. 2015. "Numerical Studies of the Outdoor Wind Environment and Thermal Comfort at Pedestrian Level in Housing Blocks with Different Building Layout Patterns and Trees Arrangement." *Renewable Energy* 73: 18–27.

Iqbal, Q. M. Z., and A. L. S. Chan. 2016. "Pedestrian Level Wind Environment Assessment Around Group of Highrise Cross-Shaped Buildings: Effect of Building Shape, Separation and Orientation." *Building and Environment* 101: 45–63.

Kato, K., and H. Huang. 2009. "Ventilation Efficiency of Void Space Surrounded by Buildings with Wind Blowing Over Built-up Urban Area." *Journal of Wind Engineering and Industrial Aerodynamics* 97: 358–367.

Lim, E., K. Ito, and M. Sandberg. 2013. "New Ventilation Index for Evaluating Imperfect Mixing Conditions - Analysis of Net Escape Velocity Based on RANS Approach." *Building and Environment* 61: 45–56.

Lin, M., J. Hang, Y. G. Li, Z. W. Luo, and M. Sandberg. 2014. "Quantitative Ventilation Assessments of Idealized Urban Canopy Layers with Various Urban Layouts and the Same Building Packing Density." *Building and Environment* 79: 152–167.

Liu, Q., and W. W. Ding. 2012. "Morphological Study on Units of Fabric That Constitute Contemporary Residential Plot in the Yangtze River Delta, China." Proceedings of the 19th International Seminar on Urban Form (ISUF), 689–694.

Liu, J. L., and J. L. Niu. 2016. "CFD Simulation of the Wind Environment Around an Isolated High-Rise Building: An Evaluation of SRANS, LES and DES Models." *Building and Environment* 96: 91–106.

Macdonald, R. W. 2000. "Modelling the Mean Velocity Profile in the Urban Canopy Layer." *Boundary-Layer Meteorology* 97 (1): 25–45.

Mei, S. J., J. T. Hua, D. Liu, F. Y. Zhao, Y. G. Li, Y. Wang, and H. Q. Wang. 2017. "Wind Driven Natural Ventilation in the Idealized Building Block Arrays with Multiple Urban Morphologies and Unique Package Building Density." *Energy and Buildings* 155: 324–338.

Memon, R. A., D. Y. C. Leung, and C. H. Liu. 2010. "Effects of Building Aspect Ratio and Wind Speed on Air Temperatures in Urban-Like Street Canyons." *Building and Environment* 45: 176–188.

Mfula, A. M., V. Kukadia, R. F. Griffithsa, and D. J. Hall. 2005. "Wind Tunnel Modelling of Urban Building Exposure to Outdoor Pollution." *Atmospheric Environment* 39: 2737–2745.

Moonen, P., V. Dorer, and J. Carmeliet. 2011. "Evaluation of the Ventilation Potential of Courtyards and Urban Street Canyons Using RANS and LES." *Journal of Wind Engineering and Industrial Aerodynamics* 99: 414–423.

Ng, E. 2009. "Policies and Technical Guidelines for Urban Planning of High-Density Cities - air Ventilation Assessment (AVA) of Hong Kong." *Energy and Buildings* 44: 1478–1488.

Ng, W. Y., and C. K. Chau. 2014. "A Modeling Investigation of the Impact of Street and Building Configurations on Personal air Pollutant Exposure in Isolated Deep Urban Canyons." *Science of the Total Environment* 468-469: 429–448.

Ng, E., C. Yuan, L. Chen, C. Ren, and J. C. H. Fung. 2011. "Improving the Wind Environment in High-Density Cities by Understanding Urban Morphology and Surface Roughness: A Study in Hong Kong." *Landscape and Urban Planning* 101: 59–74.

Oke, T. R. 1988. "Street Design and Urban Canopy Layer Climate." *Energy and Buildings* 11: 103–113.

Peng, S. H., and L. Davidson. 1997. "Towards the Determination of Regional Purging Flow Rate." *Building and Environment* 32 (6): 513–525.

Ramponi, R., B. Blocken, L. B. de Coo, and W. D. Janssen. 2015. "CFD Simulation of Outdoor Ventilation of Generic Urban Configurations with Different Urban Densities and Equal and Unequal Street Widths." *Building and Environment* 92: 152–166.

Razak, A. A., A. A. Hagishima, N. Ikegaya, and J. Tanimoto. 2013. "Analysis of Airflow Over Building Arrays for Assessment of Urban Wind Environment." *Building and Environment* 59: 56–65.

Richards, P. J., and R. P. Hoxey. 1993. "Appropriate Boundary Conditions for Computational Wind Engineering Models Using the k-ϵ Turbulence Model." *Journal of Wind Engineering and Industrial Aerodynamics* 46-47: 145–153.

Salim, S. M., R. Buccolieri, A. Chan, and S. Di Sabatino. 2011. "Numerical Simulation of Atmospheric Pollutant Dispersion in an Urban Street Canyon: Comparison Between RANS and LES." *Journal of Wind Engineering and Industrial Aerodynamics* 99: 103–113.

Shen, J. L., Z. Gao, W. W. Ding, and Y. Yu. 2017. "An Investigation on the Effect of Street Morphology to Ambient air Quality Using six Real-World Cases." *Atmospheric Environment* 164: 85–101.

Simoëns, S., and J. M. Wallace. 2008. "The Flow Across a Street Canyon of Variable Width—Part 2: Scalar Dispersion From a Street Level Line Source." *Atmospheric Environment* 42: 2489–2503.

Tominaga, Y., A. Mochida, T. Shirasawa, R. Yoshie, H. Kataoka, K. Harimoto, and T. Nozu. 2004. "Cross Comparisons of CFD Results of Wind Environment at Pedestrian Level Around a High-Rise Building and Within a Building Complex." *Journal of Asian Architecture and Building Engineering* 3 (1): 63–70.

Tominaga, Y., A. Mochida, R. Yoshie, H. Kataoka, H. Nozue, M. Yoshikawa, and T. Shirasawa. 2008. "AIJ Guidelines for Practical Applications of CFD to Pedestrian Wind Environment Around Buildings." *Journal of Wind Engineering and Industrial Aerodynamics* 96: 1749–1761.

Tominag, Y., and T. Stathopoulos. 2010. "Numerical Simulation of Dispersion Around an Isolated Cubic Building: Model Evaluation of RANS and LES." *Building and Environment* 45: 2231–2239.

Toparlar, Y., B. Blocken, B. Maiheub, and G. J. F. van Heijst. 2017. "A Review on the CFD Analysis of Urban Microclimate." *Renewable and Sustainable Energy Reviews* 80: 1613–1640.

Xie, X. M., Z. Huang, and J. S. Wang. 2006. "The Impact of Urban Street Layout on Local Atmospheric Environment." *Building and Environment* 41: 1352–1363.

Yang, F., Y. W. Gao, K. Zhong, and Y. M. Kang. 2016. "Impacts of Cross-Ventilation on the air Quality in Street Canyons with Different Building Arrangements." *Building and Environment* 104: 1–12.

Ying, X. Y., W. Zhu, K. Hokao, and J. Ge. 2013. "Numerical Research of Layout Effect on Wind Environment Around High-Rise Buildings." *Architectural Science Review* 56: 272–278.

You, W., and W. W. Ding. 2016. "*Assessment of Outdoor Space's Ventilation Efficiency Around Residential Building: Effects of Building Dimension, Separation and Orientation*." *Proceedings of 50th international conference of the Architectural Science Association (ASA 2016)*, Australia,7-9 December 2016, 219–228.

You, W., Z. Gao, Z. Chen, and W. W. Ding. 2017. "Improving Residential Wind Environments by Understanding the Relationship Between Building Arrangements and Outdoor Regional Ventilation." *Atmosphere* 8: 102.

Yuan, C., and E. Ng. 2012. "Building Porosity for Better Urban Ventilation in High-Density Cities - A Computational Parametric Study." *Building and Environment* 50: 176–189.

Yuan, C., E. Ng, and L. K. Norford. 2014. "Improving air Quality in High-Density Cities by Understanding the Relationship Between Air Pollutant Dispersion and Urban Morphologies." *Building and Environment* 71: 245–258.